

Microscopic aspects of γ softness in atomic nuclei

Stefan Frauendorf^{1,*}, Gowhar Bhat^{2,3}, Nazira Nazir⁴, Niyaz Rather⁵, Syed Rouoof⁵, Sheikh Jehangir⁵, and Javid Sheikh⁴.

¹Department of Physics and Astronomy, University of Notre Dame, Notre Dame, Indiana 46556, USA

²Department of Physics, SP College Srinagar, Jammu and Kashmir, 190 001, India

³Cluster University Srinagar, Jammu and Kashmir, Srinagar, Goji Bagh, 190 008, India

⁴Department of Physics, University of Kashmir, Srinagar, 190 006, India

⁵Department of Physics, Islamic University of Science and Technology, Awantipora, 192 122, India

Abstract. It is demonstrated that the Triaxial Projected Shell Model reproduces the energies and transition probabilities of the nucleus ^{104}Ru and the rigid triaxial nucleus ^{112}Ru . An interpretation in terms of band mixing is provided.

My presentation covers published work [1, 2], a paper under review [3] and ongoing work [4]. I start with discussing the concept of γ softness vs. γ rigidity and the corresponding observables in the traditional framework of a phenomenological Bohr Hamiltonian. Then I sketch the Triaxial Projected Shell Model (TPSM) and compare calculations for $^{104,122}\text{Ru}$ with experiment. Finally I discuss the TPSM interpretation of the appearance γ softness or γ rigidity, which is an alternative perspective traditional concept of a collective Hamiltonian.

The notation of γ softness came into use in the context of the Bohr Hamiltonian (BH) which describes collective states of the quadrupole distortion of the nuclear surface [5], where the parameter β describes the deformation and γ the triaxiality. The simple Gamma Rotor Hamiltonian of Ref. [6] is one possibility to quantify the concept of γ softness. The deformation β is assumed to be fixed. The scaled BH in the γ degree of freedom

$$\hat{\Lambda}^2 + V(\gamma) = \hat{\Lambda}^2 - \chi \cos 3\gamma + \xi \cos^2 3\gamma \quad (1)$$

contains a potential determined by the parameters χ and ξ and a kinetic term

$$\hat{\Lambda}^2 = -\left(\frac{1}{\sin 3\gamma} \frac{\partial}{\partial \gamma} \sin 3\gamma \frac{\partial}{\partial \gamma} - \frac{1}{4} \sum_{i=1,2,3} \frac{\hat{L}_i^2}{\sin^2(\gamma - \frac{2}{3}\pi i)}\right), \quad (2)$$

which is the sum of the γ kinetic energy and the rotational energy.

Fig. 1 shows examples of various potentials, which illustrate the notations of rigid vs. soft and triaxial vs. axial. Tab. 1 lists the main characteristics of the collective mode. The position of the minimum (maximum) of the potentials γ_m quantifies the degree of triaxiality. The softness of the potentials $\Delta\gamma$ is quantified as the length of the bar $E(0_1^+) < V(\gamma)$, which is a measure of the ground-state

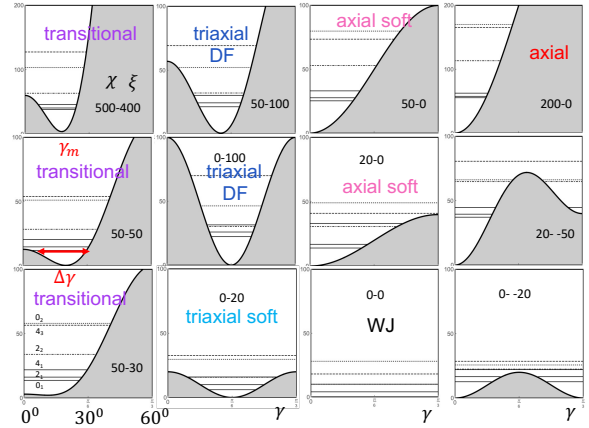


Figure 1. Selection of potentials given by Eqn. (1). The potential parameters are included as χ - ξ . The energies of the lowest states are shown as horizontal lines, where the line type indicates the I_n of the state (see the panel 50-30). The potential minimum at γ_m is a measure of the triaxiality and the width $\Delta\gamma$ is a measure how soft the potential is. To simplify terminology, "axial" or "triaxial" denote the cases with a small width. DF stands for the approach to rigid triaxial rotor (Dawydov-Fillipov limit) and WJ for the γ independent case (Wilet-Jean). Modified from Ref. [3].

fluctuation in γ . The next two columns list important energy criteria, which characterize the nature of triaxiality, namely the ratios $\left[\frac{E(2_2^+)}{E(2_1^+)}, \left[\frac{E(2_3^+)}{E(4_1^+)}\right]\right]$.

The staggering parameter $S(I)$ of the γ band is an essential observable indicating the γ softness [7].

$$S(I) = [E(I) - 2E(I-1)] + E(I-2)/E(2_1^+), \quad (3)$$

$$\bar{S}(I) = [S(I) - S(I+1)]/2. \quad (4)$$

The odd- I -down pattern indicates the concentration of the collective wave function around a finite γ -value (static triaxiality), whereas the even- I -down pattern points to a

*e-mail: sfrauend@nd.edu

Table 1. Triaxiality characteristics of the potentials plotted in Fig. 1. The staggering parameter $\bar{S}(I)$ is defined by Eq. (4). The excitation energy $E(2_1^+)_{GR}$ is the difference $E(2_1^+) - E(0_1^+)$ of the eigenvalues of the Gamma Rotor Hamiltonian (1).

$\chi - \kappa$	$E(2_1^+)_{GR}$	γ_m	$\Delta\gamma$	$\frac{E(2_1^+)}{E(2_1^+)}$	$\frac{E(2_1^+)}{E(4_1^+)}$	$\bar{S}(6)$	$Q(2_1^+)$	$B(E2, 2_2^+ \rightarrow 0_1^+)$
100-0	2.24	0	17	18.0	3.31	-0.14	-0.878	0.047
50-0	2.39	0	20	11.6	3.55	-0.51	-0.861	0.064
20-0	2.87	0	24	5.82	1.93	-1.75	-0.797	0.079
0-0	4.00	30	60	2.50	1.00	-2.75	0.000	0.000
0-200	3.05	30	16	2.11	0.81	3.87	0.000	0.000
0-100	3.57	30	19	2.21	0.86	3.12	0.000	0.000
0-20	3.95	30	22	2.45	0.98	0.50	0.000	0.000
50-100	3.10	25	19	3.50	1.20	1.85	-0.693	0.084
500-400	2.34	17	15	10.8	3.17	0.32	-0.861	0.066
50-30	2.58	11	26	7.78	2.44	-0.35	-0.835	0.082
0- -20	3.39	30	35	2.42	0.96	-5.79	0.000	0.000
20- -50	2.35	34	17	11.74	3.62	-5.55	-0.868	0.032

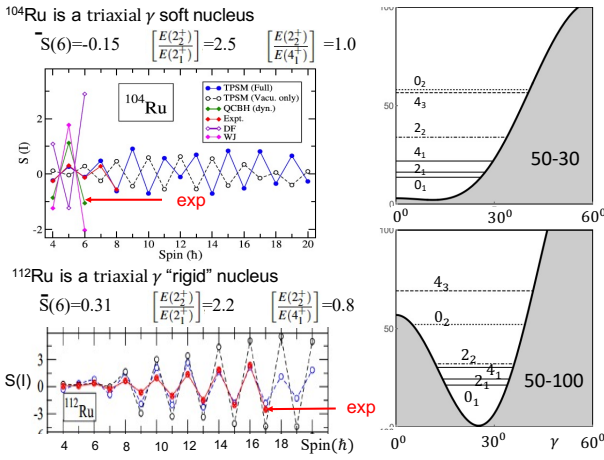


Figure 2. Phenomenological potentials (see Fig. 1) which best reproduce the shown experimental signatures of triaxiality in $^{104,112}\text{Ru}$ (see Tab. 1). Combination from Refs. [1–4].

spread of the wave function over a large range of γ (dynamic triaxiality). Tab. 1 lists the modified staggering parameter $\bar{S}(6)$.

Fig. 2 shows the experimental signatures of triaxiality in $^{104,112}\text{Ru}$. Added are the two potentials from Fig. 1, which according to Tab. 1 provide the best description of the energetic characteristics. Clearly, ^{104}Ru is a very γ soft nucleus while the triaxial shape is well established in ^{112}Ru .

The details of the TPSM are described in Refs. [1–4]. The basic methodology of the TPSM approach is similar to that of the standard spherical shell model with the exception that angular-momentum projected deformed basis is employed to diagonalize the shell model Hamiltonian. The Hamiltonian consists of monopole pairing, quadrupole pairing, and quadrupole-quadrupole interaction terms within the configuration space of three major oscillator shells ($N = 3, 4, 5$ for neutrons and $N = 2, 3, 4$ for protons)

$$\hat{H} = \hat{H}_0 - \frac{1}{2}\chi \sum_{\mu} \hat{Q}_{\mu}^{\dagger} \hat{Q}_{\mu} - G_M \hat{P}^{\dagger} \hat{P} - G_Q \sum_{\mu} \hat{P}_{\mu}^{\dagger} \hat{P}_{\mu}, \quad (5)$$

where \hat{H}_0 is the spherical single-particle potential [5]. The pairing constant G_M is determined by the BSC relation $G_M \langle \hat{P} \rangle = \Delta$. The quadrupole pairing strength G_Q is assumed to be 0.18 times G_M . The QQ-force strength χ is obtained by the self-consistency relation $2\hbar\omega\varepsilon = 3\chi \langle \Phi | \hat{Q}_0 | \Phi \rangle$. The shell model Hamiltonian (5) is diagonalized in the space of angular-momentum projected multi-quasiparticle configurations generated by the triaxial version of the Nilsson Hamiltonian [5] with the deformation parameters ε and γ . The basis is composed of the 0-qp vacuum, the two-quasiproton, the two-quasineutron and the combined four-quasiparticle configurations

$$\hat{P}_{MK}^I |\Phi\rangle, \hat{P}_{MK}^I a_{p_1}^{\dagger} a_{p_2}^{\dagger} |\Phi\rangle, \hat{P}_{MK}^I a_{n_1}^{\dagger} a_{n_2}^{\dagger} |\Phi\rangle, \hat{P}_{MK}^I a_{p_1}^{\dagger} a_{p_2}^{\dagger} a_{n_1}^{\dagger} a_{n_2}^{\dagger} |\Phi\rangle, \quad (6)$$

The TPSM has $\Delta_{p,n}$, ε and γ as input parameters. The pairing gaps $\Delta_{p,n}$ are chosen such that the overall observed odd-even mass differences are reproduced for nuclei in the considered region. The deformation parameter ε is taken from $B(E2, 2_1^+ \rightarrow 0_1^+)$ systematics or mean field equilibrium deformations. The triaxiality parameter γ is adjusted to reproduce the γ band head energy $E(2_2^+)$.

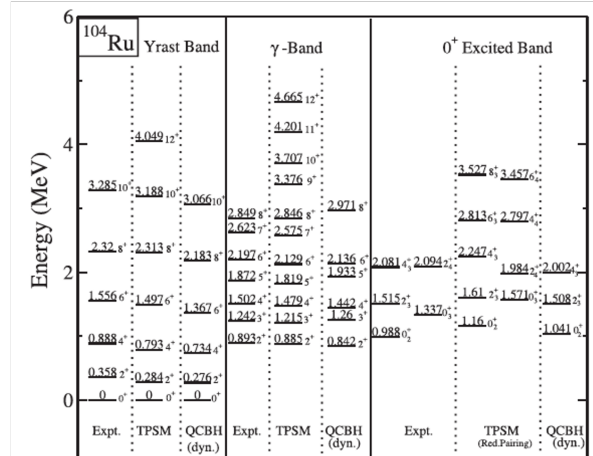


Figure 3. Comparison of the experimental levels of ^{104}Ru with the calculations by means of the TPSM and the microscopic Bohr Hamiltonian [8] (QCBH dyn). From Ref. [2].

Fig. 3 demonstrates that the TPSM very well reproduces the experimental energies of the ground, γ and excited 0^+ bands. In particular, the even-odd pattern of the staggering parameter $S(I)$ of the γ band is quantitatively reproduced, which is the energy signature γ softness (see Fig. 2). Tables 2, 3 compare the TPSM with the large number of reduced $E2$ and M matrix element measured in the COULEX experiment of Ref. [8]. The agreement of the TPSM results with the COULEX data is remarkable, because the $E2$ matrix elements provide the most direct information on the statics and dynamics of the collective quadrupole modes. Comparing the "Full" matrix elements with "Vacu." ones shows that the quasiparticle admixtures generate substantial shifts that generate the good agreement with the experiment.

Table 2. Comparison of all known experimental reduced $E2$ diagonal, in-band and inter-band matrix elements $\langle I_i || E2 || I_f \rangle$ (*e.b.*), (associated errors in parenthesis) and calculated ones for yrast- and γ -band of ^{104}Ru . From Ref. [2].

$I_i \rightarrow I_f$	Expt.	TPSM (Full)	TPSM (Vacu.)	$I_i \rightarrow I_f$	Expt.	TPSM (Full)	TPSM (Vacu.)
$2_1 \rightarrow 2_1$	-0.71(11)	-0.817	-0.634	$4_2 \rightarrow 3_1$	$\pm 0.68(5)$	-0.787	-0.597
$4_1 \rightarrow 4_1$	-0.79(15)	-0.906	-0.437	$5_1 \rightarrow 3_1$	1.22(4)	1.184	0.697
$6_1 \rightarrow 6_1$	-0.70($^{+30}_{-20}$)	-0.868	-0.342	$6_2 \rightarrow 4_2$	1.52(12)	1.521	0.682
$8_1 \rightarrow 8_1$	-0.6($^{+5}_{-5}$)	-0.855	-0.297	$8_2 \rightarrow 6_2$	2.02(4)	2.056	0.747
$2_2 \rightarrow 2_2$	0.62(8)	0.648	0.633	$2_2 \rightarrow 0_1$	-0.156(2)	-0.141	-0.225
$4_2 \rightarrow 4_2$	-0.58(18)	-0.749	-0.534	$2_2 \rightarrow 2_1$	-0.75(4)	-0.722	-0.612
$6_2 \rightarrow 6_2$	$\pm 1.0(3)$	-1.105	-0.763	$2_2 \rightarrow 4_1$	$\epsilon [-0.1, 0.1]$	-0.090	-0.001
$2_1 \rightarrow 0_1$	0.917(25)	0.973	0.901	$3_1 \rightarrow 2_1$	0.22(10)	0.254	0.302
$4_1 \rightarrow 2_1$	1.43(4)	1.591	1.456	$3_1 \rightarrow 4_1$	-0.57	-0.517	-0.559
$6_1 \rightarrow 4_1$	2.04(8)	2.081	1.830	$4_2 \rightarrow 2_1$	-0.107(8)	-0.113	-0.054
$8_1 \rightarrow 6_1$	2.59($^{+24}_{-20}$)	2.486	1.902	$4_2 \rightarrow 4_1$	-0.83(5)	-0.840	-0.505
$10_1 \rightarrow 8_1$	2.7(6)	2.668	1.623	$6_2 \rightarrow 4_1$	-0.22($^{+6}_{-12}$)	-0.230	-0.682
$3_1 \rightarrow 2_2$	-1.22(10)	-1.241	-0.935	$6_2 \rightarrow 6_1$	> -0.84	-0.947	-0.411
$4_2 \rightarrow 2_2$	1.12(5)	1.095	0.510				

Table 3. Comparison of all known experimental reduced $E2$ matrix elements $\langle I_i || E2 || I_f \rangle$ (*e.b.*), diagonal, in-band and inter-band values (associated errors in parenthesis) and calculated ones for excited 0^+ bands of ^{104}Ru . From Ref. [2].

$I_i \rightarrow I_f$	Expt.	TPSM	$I_i \rightarrow I_f$	Expt.	TPSM
$2_3 \rightarrow 0_2$	0.71(4)	0.682	$2_3 \rightarrow 4_1$	-0.370(4)	-0.311
$4_3 \rightarrow 2_3$	0.75(25)	0.613	$2_3 \rightarrow 2_2$	± 0.22 ($^{+25}_{-5}$)	-0.237
$0_2 \rightarrow 2_1$	-0.266(8)	-0.221	$2_3 \rightarrow 4_2$	0.31($^{+13}_{-14}$)	0.221
$0_2 \rightarrow 2_2$	0.08(3)	0.099	$2_3 \rightarrow 4_4$	0.53($^{+32}_{-12}$)	0.481
$2_3 \rightarrow 0_1$	-0.071(3)	-0.048	$0_3 \rightarrow 2_1$	> -0.1	-0.201
$2_3 \rightarrow 2_1$	$\pm 0.07(3)$	-0.031	$2_3 \rightarrow 2_3$	-0.08($^{11}_{-25}$)	-0.631

Figs. 4 and 5 depict the quadrupole shape invariants [9] and their dispersions calculated from the reduced $E2$ matrix elements. The invariant $\langle I_n^+ | Q^2 | I_n^+ \rangle$ measures the average intrinsic deformation of a state I_n^+ . The invariant $\langle I_n^+ | \cos 3\delta | I_n^+ \rangle$ contains the information about the triaxiality of the intrinsic shape, where $\delta = \arctan \langle I_n^+ | \cos 3\delta | I_n^+ \rangle$. The invariant Q is approximately proportional to β , and the invariant δ is approximately equal to γ of the liquid drop model [5].

The ground-band TPSM values of $\langle \cos 3\delta \rangle \sim 0.5$ in Fig. 4 signify a substantial triaxiality with preference for prolate shape, corresponding to $\gamma \approx 20^\circ$. The TPSM dispersion $\sigma \langle \cos 3\delta \rangle \sim 0.3$ indicates large fluctuations of the triaxiality parameter with 70% of the distribution within the range $9^\circ < \gamma < 24^\circ$. Hence, the TPSM shape invariants imply that ^{104}Ru is γ soft, which is in accordance with the experimental staggering parameter $S(I)$ and $\bar{S}(6) = -0.15$ in Fig. 2.

The shape invariants for ^{112}Ru in Fig. 5 correspond to narrow distributions of 7° width centered at $\gamma \approx 26^\circ$ for the ground band and $\gamma \approx 20^\circ$ for the γ band. They indicate a well established triaxial shape, which is consistent with the experimental even -I- up pattern of $S(I)$ and $\bar{S}(6) = 0.31$ in Fig. 2.

The TPSM provides an alternative perspective on the experimental signatures of γ softness. The staggering parameter of the γ band is an important signature. Fig. 6 displays the energies of the projected quasiparticle configurations in ^{104}Ru . Diagonalizing the Hamiltonian within this basis generates repulsions between neighboring states.

The $K = 2$ vacuum sequence, associated with the γ band, shows the even-I-down pattern. Mixing it with the

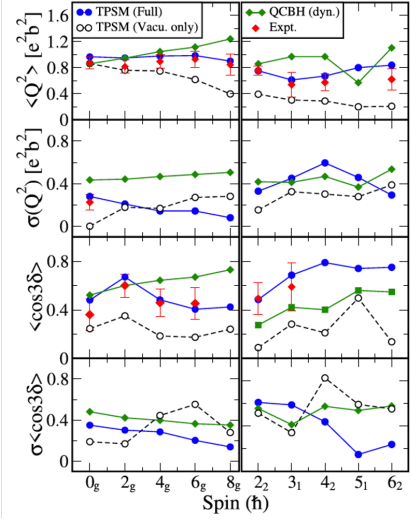


Figure 4. Comparison of the observed (Expt.) with the TPSM shape invariants for the ground-band (left panels) and γ -band (right panels) in ^{104}Ru . The results from the microscopic Bohr Hamiltonian [8] (QCBH dyn.) are included. From Ref. [2].

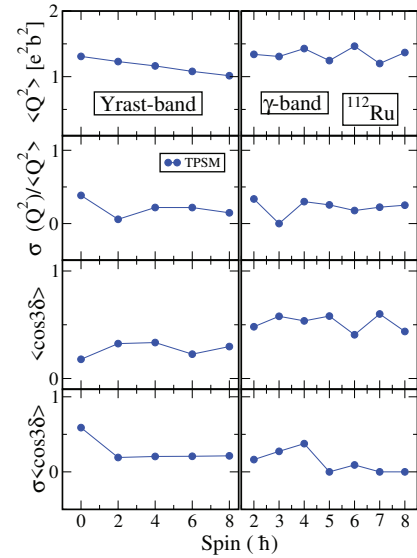


Figure 5. As Fig. 4 for ^{112}Ru . From Ref.[4].

$K = 0$ vacuum states, associated with the ground band, pushes the even -I states of the $K = 2$ band up. There is no shift for odd I, because the ground band contains only even-I states (see black arrows in Fig. 6). The triaxial rotor even-I-up pattern emerges for sufficiently strong interaction. This is the TPSM result when the basis is truncated to the K states projected from zero quasiparticle state, which is shown as "Vacu. only" (black dashed) in Fig. 2. The same even-I-up are results found for "Vacu. only" for all 35 studied nuclei [1, 2].

Admixing the lowest projected two quasiparticle states $(2\pi, 1, 1.92)$ (see purple arrows in Fig. 6) and $(2\nu, 1, 3.05)$ pushes the even-I states of the $K = 2$ vacuum

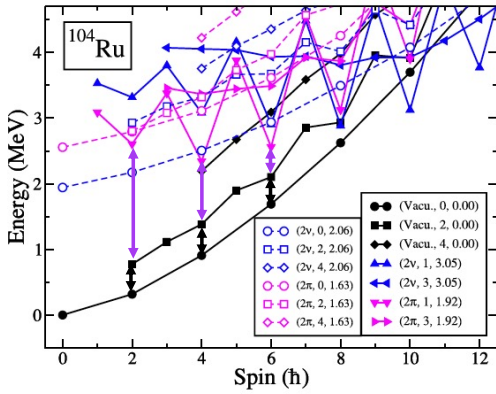


Figure 6. TPSM projected energies before band mixing. The bands are labelled by three quantities : quasiparticle character, K -quantum number and energy of the two-quasiparticle state. For instance, $(2\pi, 1, 1.92)$ designates the $K = 1$ state projected from the $h_{11/2}$ two-quasiproton configuration with the energy of 1.92 MeV. The $K = 0, 2, 4$ states projected from the quasiparticle vacuum are labelled with Vacu. The four-quasiparticle states lie above 5 MeV. The black arrows indicate the repulsion by the coupling to the ground band and the purple arrows the repulsion by coupling to the even states of the $(2\pi, 1, 1.92)$ band after band mixing. Modified from Ref. [2].

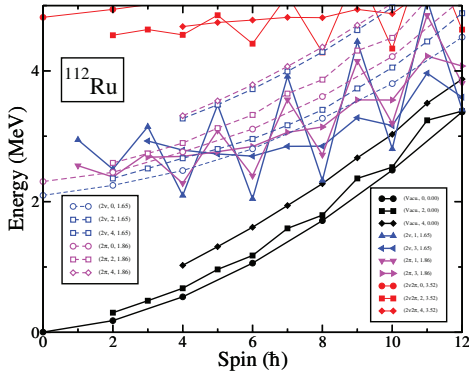


Figure 7. As Fig. 6 for ^{112}Ru . From Ref. [4].

sequence down. There is less repulsion for odd I because of the larger distance. This repulsion prevails over the one by the ground band, and the triaxial rotor pattern changes to the γ soft pattern even- I -down. The pattern flip is seen in Fig. 2 as the opposite staggering phases of the "Full" results (blue dashed) compared to the "Vacu. only" (black dashed) ones.

Fig. 7 displays the energies of the projected quasiparticle configurations in ^{112}Ru . The distance between the $K = 2$ and $K = 0$ sequences projected from the vacuum is much smaller than for ^{104}Ru . Their mixing is stronger and the corresponding shift is larger. It prevails over the downshift by the repulsion of the two-quasiparticle sequences, such the staggering amplitude is reduced but its phase remains unchanged (see Fig. 2).

The competition between the two kinds of band mixing accounts for the observed $S(I)$ pattern for the 35 nu-

clides studied in Refs. [1–4]. The mixing with the two-quasiparticle states provides a natural explanation for the observed rapid change of the $S(I)$ with N and Z , because the quasiparticle structure near the Fermi level plays a central role. The mixing interpretation explains also the $Z - N$ dependence of the triaxiality characteristics of transition probabilities [3].

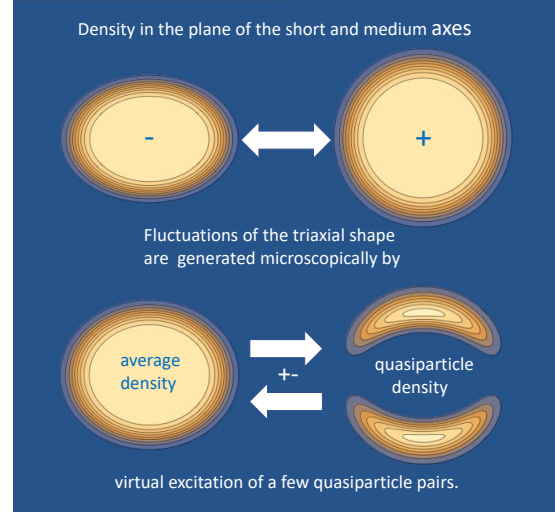


Figure 8. Summary: One of the main research themes in quantum many-body systems is the emergence of collective features from microscopic degrees of freedom. Using the microscopic approach of the triaxial projected shell model, the authors demonstrate that admixing a few quasiparticle excitations into the vacuum configuration with a fixed triaxiality parameter γ provides a quantitative description of the shape fluctuations of the γ -soft nucleus ^{104}Ru . The collective features are elucidated using the quadrupole shape invariant analysis, and also the staggering phase classification of the γ band. Figure and text from the editor's suggestion in Phys. Rev. C 107, Issue 2, (2023).

References

- [1] S. Jehangir, G.H. Bhat, J.A. Sheikh, S. Frauendorf, W. Li, R. Palit, N. Rather, Eur. Phys. J. A **57**, 308 (2021).
- [2] S.P. Rouoof, Nazira Nazir, S. Jehangir, G.H. Bhat, J.A. Sheikh, N. Rather, S. Frauendorf, Phys. Rev. C **107**, L021303 (2023).
- [3] S.P. Rouoof, Nazira Nazir, S. Jehangir, G.H. Bhat, J.A. Sheikh, N. Rather, S. Frauendorf, Eur. Phys. J. A, in revision, arXiv:2307.06670.
- [4] S.P. Rouoof, S. Jehangir, Nazira Nazir, G.H. Bhat, J.A. Sheikh, N. Rather, S. Frauendorf, Eur. Phys. J. A, in preparation.
- [5] A. Bohr and B. R. Mottelson, *Nuclear Structure, Vol. II* (Benjamin Inc., New York, 1975).
- [6] M. A. Caprio, Phys. Rev. C **83**, 064309 (2011).
- [7] N. V. Zamfir and R. F. Casten, Phys. Lett. B **3**, 260 (1991).
- [8] K. Zajac, L. Próchniak, K. Pomorski, S.G. Rohoziński and J. Srebrny, Nucl. Phys. A **653**, 71 (1999).
- [9] D. Cline, Ann. Rev. of Nucl. and Part. Science, **36**, 683 (1986).

